Residual Synchronization Error Elimination in OFDM Baseband Receivers

Xingbo Hu, Yumei Huang, and Zhiliang Hong

It is well known that an OFDM receiver is vulnerable to synchronization errors. Despite fine estimations used in the initial acquisition, there are still residual synchronization errors. Though these errors are very small, they severely degrade the bit error rate (BER) performance. In this paper, we propose a residual error elimination scheme for the digital OFDM baseband receiver aiming to improve the overall BER performance. Three improvements on existing schemes are made: a pilot-aided recursive algorithm for joint estimation of the residual carrier frequency and sampling time offsets; a delay-based timing error correction technique, which smoothly adjusts the incoming data stream without resampling disturbance; and a decision-directed channel gain update algorithm based on recursive least-squares criterion, which offers faster convergence and smaller error than the least-mean-squares algorithms. Simulation results show that the proposed scheme works well in the multipath channel, and its performance is close to that of an OFDM system with perfect synchronization parameters.

Keywords: OFDM, error elimination, offset estimation, timing error correction, channel gain update.

I. Introduction

The digital baseband receiver, one of the key parts in an OFDM system, plays an important role in determining the overall transmission performance. Design and implementation of the OFDM receiver have been topics of intense activity for researchers and engineers since OFDM was invented. Numerous papers have been published to address issues concerning OFDM receiver design, including the issue of synchronization for received signals. An OFDM system is very vulnerable to synchronization errors and there are more stringent requirements for synchronization tasks in an OFDM receiver than in others. In addition to the initial estimation for synchronization parameters, further elimination of residual synchronization errors (including carrier-frequency and timing errors or offsets) is absolutely necessary. The absence of an efficient error elimination scheme in the OFDM receiver would severely degrade the overall system performance. Obviously, how to design an efficient and robust elimination scheme for residual synchronization errors is a critical issue while implementing a digital OFDM receiver.

Error elimination is mainly composed of two processing tasks, error estimation and error correction [1]-[3]. Various algorithms have been proposed to estimate both the carrier frequency offset (CFO) and the sampling time offset (STO) using phases or phase differences of signals at pilot subcarriers [1], [4]-[6]. Underlying these algorithms is the least-squares (LS) line-fitting method [5] or its weighted version [6]. In order to obtain good estimation accuracy, the number of pilot subcarriers per OFDM symbol should be large enough; otherwise, for many burst-type OFDM systems (such as IEEE 802.11a/g WLANs and 802.16d/e BWA systems), due to very limited number of pilot subcarriers per OFDM symbol, phase

Manuscript received Feb. 07, 2007; revised May 11, 2007.

This work was supported in part by Intel Research Council and in part by the Applied Materials Shanghai Research & Development Fund under grant no. 0507.

Xingbo Hu (phone: + 86 21 5135 5268, email: xbhu@fudan.edu.cn), Yumei Huang (email: yumeihuang@fudan.edu.cn), and Zhiliang Hong (email: zlhong@fudan.edu.cn) are with the State Key Laboratory of ASIC and Systems, School of Microelectronics, Fudan University, Shanghai, P.R. China.

differences have to be averaged over many OFDM symbols for the sake of noise suppression. However, averaging across many symbols calls for large data storage and slows down the estimator's response to diminishing residual errors.

Error correction is also indispensable for an error elimination scheme. A time or frequency domain phase derotator is widely used to correct carrier-frequency errors [2], [7]. As for timing error correction, it can be performed by adjusting a resampling numerically-controlled oscillator (NCO) [1], [8]. However, this timing error correction design ignores that the drifting timing phase caused by the STO would jump beyond sample boundaries to induce either sample stuffing or rubbing. The large sampling disturbance could crash the signal detection.

In this paper, we present an efficient residual synchronization error elimination scheme for the digital OFDM baseband receiver. It deals with the CFO and STO induced phase rotation effects and also random phase noises, aiming to improve the overall bit error rate (BER) performance via fine tracking of residual synchronization errors and efficient digital error compensation. It has the canonical architecture described in [1] and [6], but three improvements on existing schemes are proposed. We do not use an averaging-based LS line-fitting method; rather, we use a new recursive least-squares (RLS) algorithm for the joint CFO and STO estimation. Instead of adopting an NCO-based timing error corrector, a delay-based correction technique is devised to resample the incoming data stream without sampling disturbance. Our proposed scheme also incorporates an effective channel tracking loop as the further error elimination stage. This channel tracking loop employs a new decision-directed effective channel gain update algorithm based on RLS criterion other than the conventional least- mean-square (LMS) criterion.

This paper is organized as follows. In section II, the OFDM signal model with synchronization imperfections is described in mathematical expressions. Next, the proposed residual error elimination scheme is briefly introduced in section III. Then, three new algorithms or techniques devised for this scheme are presented in detail in section IV. Simulation results demonstrating the performance of the proposed scheme are given in section V. Finally, section VI concludes this paper.

II. OFDM Signal Model with Synchronization Imperfections

Consider an OFDM system using N-point inverse fast Fourier transform (IFFT) and FFT for modulation and demodulation, respectively, as shown in Fig. 1. Each OFDM symbol is composed of K_u ($< N$) data symbols $X_{i,k}$, where i denotes the OFDM symbol time index, and k denotes the subcarrier frequency index. The output of the IFFT is discrete time with sampling time $T = T_u / N$, where T_u is the duration of an OFDM symbol's useful part. Thus, according to [9], the baseband complex envelope for the transmitted OFDM signal can be expressed as

$$x(t) = \sum_{i=-\infty}^{\infty} \sum_{k=-K_u/2}^{K_u/2} X_{i,k} \cdot e^{j2\pi(k/T_u)(t-T_g-iT_s)} \cdot u(t-iT_s), \quad (1)$$

where T_s is the duration of an OFDM symbol, T_g is the duration of the guard interval (or cyclic prefix, CP) in an OFDM symbol, and $u(t)$ is the rectangular pulse shape function with unit amplitude during $0 \le t \le T_s$.

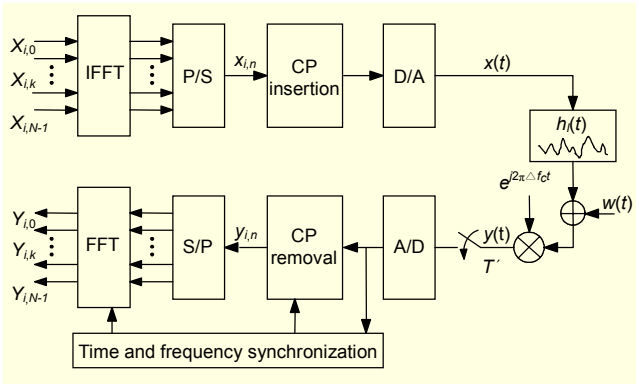

Fig. 1. Baseband transmission model for an OFDM system.

The transmitted signal is corrupted in a multipath fading channel with additive white Gaussian noise (AWGN). At the receiver side, the complex baseband signal is given as in [9] by

$$y(t) = \sum_{l=1}^{L} h_l(t) \cdot x(t-\tau_l) + w(t), \quad (2)$$

where L is the total number of paths; $h_l(t)$ and τ_l denote the complex gain and delay of the l-th path, respectively; and $w(t)$ is the additive white Gaussian noise.

The receiver samples the signal $y(t)$ with the time interval of T'. Due to the existing frequency difference between transmitter and receiver oscillators, the received n-th time-domain sample of the i-th OFDM symbol is given by

$$y_{i,n} = e^{j2\pi\Delta f_C t} \cdot y(t)\big|_{t=(n+N_g+i\cdot N_{sym})T'} \quad (n = -N_g, \cdots, N-1), \quad (3)$$

where N_{sym} is the length of an OFDM symbol, N_g is the length of the cyclic prefix, and Δf_C denotes the carrier frequency offset. Then, synchronization, CP stripping, and FFT demodulation are performed sequentially on the received signal. If the synchronization process is perfect, we can have the received complex frequency-domain data on the k-th subcarrier of the i-th symbol $Y_{i,k}$ as

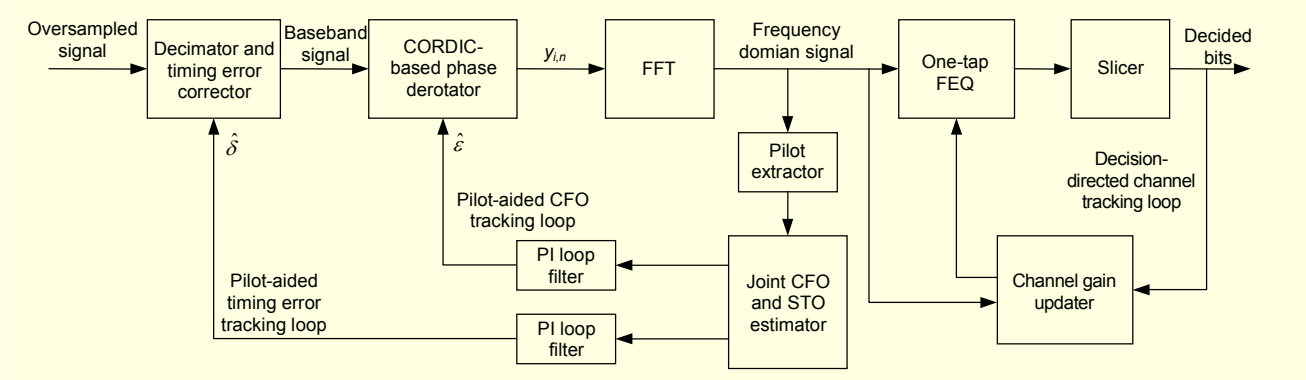

Fig. 2. Architecture of the proposed residual synchronization error elimination.

$$Y_{i,k} = X_{i,k} \cdot H_{i,k} + W_{i,k}, \tag{4}$$

where $W_{i,k}$ is the complex additive noise on the corresponding subcarrier, and $H_{i,k}$ is the channel frequency response given by

$$H_{i,k} = \sum_{l=1}^{L} h_l(iT_s) \cdot e^{-j2\pi k(\tau_l / T_u)}. \tag{5}$$

However, in practical systems, there is no ideal synchronization, and very small CFO will remain even after the finest estimation process. Furthermore, the STO induced timing error will also cause disturbances in the receiver. If some residual carrier frequency offset $\varepsilon\Delta f$ (Δf denotes the subcarrier frequency spacing) and sampling time offset δT exist, the received symbol $Y_{i,k}$ consists of a signal term $S_{i,k}$, an inter-carrier interference (ICI) $I_{i,k}$, and a noise term $W_{i,k}$ [6]

$$Y_{i,k} = S_{i,k} + I_{i,k} + W_{i,k}. \tag{6}$$

As given in [6], the frequency offset parameter (ϕ_{qk}), the signal term ($S_{i,k}$), and the interference term ($I_{i,k}$) can be expressed as

$$\phi_{qk} = (1+\delta) \cdot (\varepsilon + q) - k, \tag{7}$$

$$S_{i,k} = X_{i,k} H_{i,k} \cdot \frac{\sin(\pi\phi_{kk})}{N \sin(\pi\phi_{kk} / N)} \cdot e^{j2\pi(iN+iN_g+N_g)\phi_{kk}/N} \cdot e^{j\pi\phi_{kk}(1-1/N)}, \tag{8}$$

$$I_{i,k} = \sum_{q=-N/2+1, q\neq k}^{N/2} X_{i,k} H_{i,k} \cdot \frac{\sin(\pi\phi_{qk})}{N \sin(\pi\phi_{qk} / N)} \cdot e^{j2\pi(iN+iN_g+N_g)\phi_{qq}/N} \cdot e^{j\pi\phi_{qk}(1-1/N)}. \tag{9}$$

III. Residual Error Elimination Scheme

As previously mentioned, both CFO and STO exist in practical OFDM systems. For an OFDM receiver, good performance is achieved only by accurate offset estimation and efficient digital compensation. However, there always remains more or less error for any estimation algorithm if noise is present in received signals. Residual synchronization errors, even if very small, will severely degrade the overall BER performance. The deleterious effects of the residual CFO and the STO-induced timing offsets on reception performance are carefully analyzed in [10]. To combat these negative effects, residual synchronization offsets must be corrected via efficient fine tracking schemes.

Figure 2 depicts the architecture of our proposed residual synchronization error elimination scheme. It is built with an FFT processor, a one-tap frequency-domain equalizer, and a slicer. It is composed of three loops: a pilot-aided timing error tracking loop, a pilot-aided carrier frequency error tracking loop, and a decision-directed channel gain tracking loop. The received baseband signals with residual synchronization errors are corrected via the pilot-aided error tracking loops. However, tiny errors (usually $|\varepsilon| \le 10^{-3}$, $|\delta| \le 10$ ppm) still exist after the fine tracking process. In our scheme, the decision-directed channel tracking loop is utilized to further eliminate the remaining tiny synchronization errors for BER performance improvement, because the channel estimator/updater cannot distinguish the small phase rotation term $e^{j\pi\phi_k}$ from the channel gain coefficients H_k $(-K_u/2 \le k \le K_u/2)$.

The whole error elimination structure consists of several building blocks: the joint CFO and STO estimator, the loop filters, the timing error corrector, the phase derotator, and the channel gain updater. The well-known CORDIC algorithm is used to implement the phase derotation. The proportional-and-integral (PI) regulator is adopted here as the loop filter in both the carrier frequency and timing tracking loops. Although our proposed architecture is similar to that in [1] or [6], three new algorithms or techniques are devised to achieve improvement over existing systems:

• *A pilot-aided recursive algorithm for joint estimation of the carrier-frequency and sampling time offsets*. Existing systems with a small number of pilots per OFDM symbol usually adopt an averaging-based LS line-fitting method or its weighted version for offset estimation [6]. This line-fitting estimator has a very slow response to changing parameters as well as a large data storage requirement. The proposed estimator is based on the RLS algorithm, which can recursively estimate residual synchronization errors in an adaptive fashion. It also requires less storage than conventional estimators.

• *A delay-based timing error correction technique*. Unlike the popular NCO-based timing error correction in [8], it can resample the incoming data stream without introducing any sampling disturbance. It is also easier to implement than existing techniques.

• *A decision-directed effective channel gain update algorithm based on the RLS criterion*. This algorithm offers faster convergence and smaller error than the conventional LMS algorithms.

IV. Proposed Algorithms and Techniques

1. Recursive Algorithm for Error Estimation

Error detection or estimation is vital for an error tracking loop since efficient correction is based on a fine estimation algorithm. An unbiased estimate with little variance is expected to be fed to the error correction unit. In the design of OFDM error tracking loops, joint estimation of the carrier frequency and sampling time offsets is preferred for the simple reason that the phase shifts of subcarriers caused by both offsets cannot be easily distinguished from each other.

As previously mentioned, an LS line-fitting algorithm is popularly utilized to estimate the CFO and STO from the extracted phase differences in the received pilot subcarrier signals between two consecutive OFDM symbols. For many OFDM systems where the number of pilot subcarriers per OFDM symbol is limited (namely, four in 802.11a systems and eight in 802.16d systems), the phase differences have to be averaged over many OFDM symbols in order to improve estimation. The more symbols used for averaging, the more accurate the estimation is, the poorer the tracking ability for dynamic parameters is, and the more memory is required (storage of all pilot subcarrier signals in OFDM symbols used for averaging cannot be avoided). There is a trade-off between accuracy and complexity as well as dynamic performance for these averaging-based LS line-fitting algorithms. In this section, we propose a pilot-aided RLS algorithm for joint estimation of CFO and STO, which can adaptively estimate dynamically decreasing residual errors in a recursive fashion. It can also achieve hardware efficiency by greatly reducing data storage while improving estimation performance of the conventional LS line-fitting algorithms.

In the appendix we show the detailed mathematical derivation of the proposed recursive algorithm. The complete algorithm is summarized in Fig. 3.

I) Initialization ($i = 0$). Set $\hat{\mathbf{b}}_0 = [0 \quad 0]^T$ and

$\mathbf{V}_0 = \rho^{-1}\mathbf{I}$ (where ρ is a small positive), then

$$[\hat{\delta}_0 \quad \hat{\varepsilon}_0]^T = \frac{N}{2\pi(N+N_g)}\hat{\mathbf{b}}_0 .$$

II) Iterative computations ($i \rightarrow i+1$, $i \geq 1$).

1) Let $\hat{\mathbf{b}}_{i+1,-1} = \hat{\mathbf{b}}_i$ and $\mathbf{V}_{i+1,-1} = \mathbf{V}_i$.

2) For $j = 0, 1, \ldots, J-1$, repeat:

a) Let $\omega_{i,j} = \left| Y_{i,p_j} / X_{i,p_j} \right|$, $\mathbf{q}_{i+1,j}^T = [\omega_{i+1,j} p_j \quad \omega_{i+1,j}]$,

$\psi_{i+1,j} = \omega_{i+1,j}\varphi_{i+1,j}$.

b) Compute:

$$\mathbf{K}_{i+1,j} = (w + \mathbf{q}_{i+1,j}^T \mathbf{V}_{i+1,j-1}\mathbf{q}_{i+1,j})^{-1}\mathbf{V}_{i+1,\ j-1}\mathbf{q}_{i+1,j},$$

$$\hat{\mathbf{b}}_{i+1,j} = \hat{\mathbf{b}}_{i+1,j-1} + \mathbf{K}_{i+1,j}(\psi_{i+1,j} - \mathbf{q}_{i+1,j}^T \ \hat{\mathbf{b}}_{i+1,j-1}),$$

$$\mathbf{V}_{i+1,j} = (\mathbf{V}_{i+1,j-1} - \mathbf{K}_{i+1,j}\mathbf{q}_{i+1,j}^T \mathbf{V}_{i+1,j-1}) \ /w,$$

where $0 < w < 1$.

3) Let $\hat{\mathbf{b}}_{i+1} = \hat{\mathbf{b}}_{i+1,J-1}$.

4) Compute the estimates of CFO and STO:

$$[\hat{\delta}_{i+1} \quad \hat{\varepsilon}_{i+1}]^T = \frac{N}{2\pi(N+N_g)}\hat{\mathbf{b}}_{i+1} .$$

Fig. 3. Recursive algorithm for joint estimation of CFO and STO.

In addition to keeping all pilot data in the last OFDM symbol for phase-difference computations, this recursive algorithm requires storage of only old values for the 2-element vector $\mathbf{b}$ and the 2-by-2 matrix $\mathbf{V}$, while conventional LS algorithms call for the unavoidable storage of $N_{av} \times J$ pilot data (N_{av} is the number of OFDM symbols used for averaging, and J denotes the pilot number in an OFDM symbol). Generally, J takes the value of 4, 8, or a larger even number. To obtain good enough results, N_{av} should be no less than 10. Obviously, large storage savings can be achieved by applying the proposed recursive algorithm in joint estimation of the carrier frequency and sampling clock offsets in digital OFDM baseband receivers.

In order to evaluate the performance of the proposed recursive algorithm, consider the mean behavior and the mean square behavior of the error vector

$$\Delta\mathbf{b}(i) = \hat{\mathbf{b}}_i - \mathbf{b}_o , \tag{10}$$

where $\mathbf{b}_o$ is the optimum value for the offset vector (also the true value since the phase noise $e_{i,j}$ is zero-mean). The expectation of the error vector can be derived from the recursive computation formulas, which is given by

$$E\{\Delta \boldsymbol{b}(i)\} = -\frac{(1-w)w^i}{\rho(1-w^i)}(\mathbf{Q}^T\mathbf{Q})^{-1}\mathbf{b}_o . \quad (11)$$

Since the forgetting factor w is a positive number less than 1, $E\{\Delta\mathbf{b}(i)\} \to 0$ as $i \to \infty$. That is to say, the mean of the estimated offset sequences can always converge to their true values. The mean-square deviation (MSD) can be expressed as

$$\begin{aligned} D(i) &= \mathrm{tr}[E\{\Delta\mathbf{b}(i)\Delta\mathbf{b}^T(i)\}] \\ &= \rho^2 \frac{(1-w)^2 w^{2i}}{(1-w^i)^2}\mathrm{tr}[(\mathbf{Q}^T\mathbf{Q})^{-1}\mathbf{b}_o\mathbf{b}_o^T(\mathbf{Q}^T\mathbf{Q})^{-1}] \\ &\quad + \sigma_o^2 \frac{(1-w)(1-w^{2i+2})}{(1+w)(1-w^i)^2}\mathrm{tr}[(\mathbf{Q}^T\mathbf{Q})^{-1}], \end{aligned} \quad (12)$$

where σ_o^2 is the minimum variance of the phase noise e_{ij}. From (12), it can be concluded that the MSD of the proposed recursive estimation algorithm decays exponentially with time.

2. Delay-Based Timing Error Correction

It is well known that timing error correction can be performed by means of interpolating among received signal samples in digital receivers [8]. Usually, the interpolator, also called an interpolating filter, is controlled by an NCO which offers information needed to perform the interpolating computations [8]. However, this conventional error correction technique would introduce resampling disturbance which could crash the signal detection. Here, we present an efficient timing error corrector based on a delay-variable buffer, which could overcome the weaknesses mentioned and also obviate the need for an NCO part.

Figure 4 is the block diagram of our proposed timing error correction structure. Since the interpolator can only adjust fractional timing error, a sample buffer with adjustable delay time and a sample manipulator adopting the skip/duplicate concept proposed in [11] are mounted before and after the interpolator, respectively, to correct the integral timing offset jointly. Control parameters or commands required by these components are provided by the timing phase controller, which derives the phase information and determines the sample

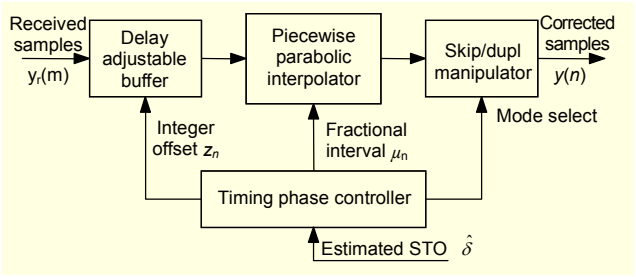

Fig. 4. Structure of the proposed timing error corrector.

alignment modes based on the estimated value of the normalized STO.

According to [8], the whole process for timing error correction can be mathematically modeled as

$$\begin{aligned} y(nT_i) &= y[(m_n + \mu_n)T_{os}'] \\ &= \sum_{i=I_1}^{I_2} y_r[(m_n - i)T_{os}'] \cdot h_I[(i+\mu_n)T_{os}'], \end{aligned} \quad (13)$$

with

$$m_n = \mathrm{int}[nT_i / T_{os}'], \quad (14)$$

$$\mu_n = nT_i / T_{os}' - m_n, \quad (15)$$

where $h_I(t)$ denotes the impulse response function of the interpolating filter, m_n is the basepoint index, μ_n is the fractional interval, T_i is the time interval between two consecutive interpolants, and T_{os}' is the oversampling period at the receiver end.

A four-point piecewise-parabolic interpolator is adopted in our proposed timing correction unit. For a given design parameter $\alpha (0 \le \alpha \le 1)$, the interpolating filter's coefficient formulas are

$$\begin{aligned} C_{-2} &= \alpha\mu^2 - \alpha\mu, \\ C_{-1} &= -\alpha\mu^2 + (\alpha+1)\mu, \\ C_0 &= -\alpha\mu^2 + (\alpha-1)\mu + 1, \\ C_1 &= \alpha\mu^2 - \alpha\mu. \end{aligned} \quad (16)$$

Since these coefficients are functions of μ_n, the interpolator can be designed using the well-known Farrow structure [12].

The timing phase controller does not use an NCO. It directly updates the integral timing offset and the fractional interval by simple computations from their old values as well as the estimate of normalized STO – $\hat{\delta}$ and makes the current information available to other components. The derivation of the recursive formulas is described here.

Two successive interpolations are performed for time instants n and n+1, and we can have the following recursion:

$$m_{n+1} + \mu_{n+1} = m_n + T_i / T_{os}' + \mu_n . \quad (17)$$

Since, by definition, $0 \le \mu_{n+1} < 1$ as given in [8], the increment in sample count from one interpolation to the next is

$$\Delta m_n = m_{n+1} - m_n = \mathrm{int}[T_i / T_{os}' + \mu_n]. \quad (18)$$

The value of T_i / T_{os}' is determined by $\hat{\delta}$. Considering that $T_i = T'/(1+\hat{\delta})$ and $T_{os}' = T'/R_{os}$, where R_{os} is the rate of over-sampling, it can be derived that

$$T_i / T_{os}' = R_{os}/(1+\hat{\delta}) . \quad (19)$$

Therefore, (18) can be rewritten as

$$\Delta m_n = \text{int}[R_{os}/(1+\hat{\delta}) + \mu_n]. \quad (20)$$

From (17) and (20), we may conclude that

$$\mu_{n+1} = \mu_n + R_{os}/(1+\hat{\delta}) - \Delta m_n. \quad (21)$$

The integral timing offset can be updated as

$$z_{n+1} = z_n + \Delta m_n - R_{os}. \quad (22)$$

Equations (20) to (22) constitute the recursive formulas for computing the integral timing offset and the fractional interval.

The delay-adjustable buffer feeds the interpolator with a continuous data stream free of effects of sampling jitters by automatically altering the delay time for output samples. When a positive integral timing offset occurs, the sample delay length is decreased. On the contrary, a negative integer offset for the received samples leads to an increase in the delay length. If there is no integral timing offset, samples are delayed by fixed clock cycles. A sample skip/duplicate manipulator mounted after the interpolator is indispensable in confining the size of the sample buffer within an acceptable range. It resets the integral timing offset by skipping or duplicating a baseband sample so that the buffer size will remain finite in non-stopping transmissions. It works in one of three modes: normal, skip, or duplicate, and this is determined by the control command issued by the timing phase controller.

The delay length for the received samples at the time instant n is given by

$$D_n = D_{fix} - z_n, \quad (23)$$

where D_{fix} is the fixed delay length when there is no integral timing offset. Assume the integer offset takes a value in the range of $[Z_{\min}, Z_{\max}]$ ($Z_{\min}$ is negative, whereas $Z_{\max}$ is positive). The sample buffer's size should be $Z_{\max} - Z_{\min}$. In order to make the buffer size as short as possible, it is necessary to confine z_n to a narrow range. For example, consider integer region $[-R_{os}, 2R_{os}-1]$. If $0 \le z_n \le R_{os}-1$, the skip/duplicate manipulator will stay in the normal mode. However, if z_n falls outside of the range $[0, R_{os}-1]$, a sample of the CP at the start of the next received OFDM symbol will be skipped or duplicated, and at the same time, the integer offset will be reset to an integer in $[0, R_{os}-1]$ by adding or subtracting R_{os} from the original offset. Since the timing phase offset accumulated during an OFDM symbol period does not exceed a baseband sample time in all OFDM systems, even for as large an STO as 100 ppm, the range of $[-R_{os}, 2R_{os}-1]$ would be wide enough to ensure proper processing.

3. Decision-Directed Channel Gain Update

A channel gain update scheme is mainly utilized to combat the deleterious effects of variations in the transmission channel. Nevertheless, it can also eliminate tiny synchronization errors remaining even after the fine offset estimation and tracking. In the following, a new decision-directed channel gain update algorithm is described in detail.

At the receiver end, the data symbol on the k-th subcarrier of the i-th OFDM symbol is given by

$$Y(i,k) = X(i,k) \cdot H_{\varepsilon}(i,k) + W(i,k), \quad (24)$$

where $X(i, k)$ is the transmitted data symbol, $W(i, k)$ is the additive white Gaussian noise, and $H_{\varepsilon}(i,k)$ is the effective channel gain coefficients incorporating the true channel frequency response and the modified phase induced by tiny synchronization errors. A one-tap frequency-domain equalizer (FEQ) equalizes the symbol $Y(i, k)$ with the estimated effective channel coefficients $\hat{H}_{\varepsilon}(i,k)$ to yield

$$X_e(i,k) = Y(i,k)/\hat{H}_{\varepsilon}(i,k). \quad (25)$$

The equalized symbol $X_e(i, k)$ is fed to the slicer for hard or soft decision and then re-mapped to yield $X_d(i, k)$. Obviously, $X_d(i, k)$ is the constellation point nearest to $X_e(i, k)$. If the receiver works properly, $X_d(i, k)$ can be regarded as the transmitted data symbol $X(i, k)$. Thus, (24) can be rewritten as

$$Y(i,k) = X_d(i,k) \cdot H_{\varepsilon}(i,k) + W(i,k). \quad (26)$$

The estimates of the effective channel gain coefficients $\hat{H}_{\varepsilon}(i,k)$ can be computed from (26) as well as its previous i equations.

In digital communication systems, the LMS algorithm is widely used in adaptive equalization due to its simplicity. However, the LMS algorithm has a slow convergence property. In our scheme, the RLS criterion is adopted to adaptively update the effective channel gain coefficients in real time since it offers faster convergence and smaller error than the LMS algorithm despite some computational complexity. The recursive computation formulas are described as follows:

$$K(i+1,k) = \frac{P(i,k) \cdot X_d^*(i+1,k)}{\lambda + X_d(i+1,k) \cdot P(i,k) \cdot X_d^*(i+1,k)}, \quad (27)$$

$$P(i+1,k) = [P(i,k) - K(i+1,k) \cdot X_d(i+1,k) \cdot P(i,k)]/\lambda, \quad (28)$$

and

$$\hat{H}_{\varepsilon}(i+1,k) = \hat{H}_{\varepsilon}(i,k) + K(i+1,k) \cdot [Y(i+1,k) - X_d(i+1,k) \cdot \hat{H}_{\varepsilon}(i,k)], \quad (29)$$

where $(\cdot)^*$ denotes conjugate operation, and the weighting coefficient λ ($0 < \lambda < 1$) is called the forgetting factor, which determines how the algorithm treats past data input to the

algorithm.

The recursive computations for the effective channel gain coefficients can start from the results of the initial channel estimation. The initial values of $P(0, k)$ can de determined by

$$P(0,k) = [X_d^*(0,k) \cdot X_d(0,k)]^{-1}. \quad (30)$$

It is difficult to perform mathematical analysis for multi-variable RLS algorithms. However, since our proposed update algorithm is a single-variable one, the performance evaluation in analytical forms becomes easier. First, evaluate its convergence property. The expectation of the estimation error for the effective channel frequency response on the k-th subcarrier during the i-th symbol period is approximated as

$$E\{\Delta H(i,k)\} \approx \frac{\lambda^i(1-\lambda)}{1-\lambda^{i+1}} \cdot \frac{\hat{R}(0,k) \cdot \Delta H(0,k)}{\sigma_x^2}, \quad (31)$$

where

$$\hat{R}(0,k) = X_d(0,k) X_d^*(0,k),$$

$$\sigma_x^2 = E\{X_d(i,k) X_d^*(i,k)\}.$$

Since $0 < \lambda < 1$, $E\{\Delta H(i,k)\} \to 0$ as $i \to \infty$ for any k. Therefore, this update process is asymptotically convergent.

Next, consider the mean square behavior for this RLS algorithm. Its MSD can be expressed as

$$D(i,k) = E\{\Delta H(i,k) \cdot \Delta H^*(i,k)\} \approx \frac{\lambda^{2i}(1-\lambda)^2}{(1-\lambda^{i+1})^2} \cdot \frac{|X(0,k)|^4}{\sigma_x^2} + \frac{(1-\lambda)(1+\lambda^{i+1})}{(1+\lambda)(1-\lambda^{i+1})} \cdot \frac{\sigma_x^2 \sigma_w^4}{\sigma_x^4}, \quad (32)$$

where σ_w^2 is the variance of the additive noise $W(i, k)$.

V. Numerical Simulations

We provide several numerical examples to demonstrate the overall system performance of using our proposed error elimination scheme. A burst-based OFDM system with reference to the IEEE 802.16d standard [13] is used in our simulations. In particular, we assume four primitive parameters characterizing the OFDM symbol defined as follows. The nominal channel bandwidth BW = 10 MHz, the number of subcarriers used N_{used} = 200, the sampling factor n = 57/50 and the ratio of CP time to useful time G = 1/8. Since the 802.16d standard is for fixed broadband wireless access applications, the SUI-4 channel model [14] with the maximum Doppler frequency of 20 Hz is adopted in our simulations. Common simulation conditions are the following:

- the packet length (that is, the number of OFDM symbols in a packet) is 200;
- the modulation types are BPSK for pilots and 16-QAM for data, respectively;
- the forgetting factor w and the value of ρ in the RLS-based residual offset estimation algorithm are set to 0.975 and 0.01, respectively;
- the forgetting factor λ in the effective channel gain update algorithm is 0.90625.

All statistical simulation results given in this section are obtained with 10^4 Monte Carlo trials.

First, some simulation trials are performed to justify the effectiveness of the pilot-aided error tracking loops. Figure 5 shows a snapshot of the residual synchronization error tracking convergence and steady-state performance at different SNR levels. The initial normalized offsets for the carrier frequency and the sampling clock are 0.01 and 50 ppm, respectively. At SNR levels of greater than 10 dB, the convergence of both CFO and STO tracking can be achieved after approximately 20 symbols, and the curves fluctuate little in the steady state. Some tracking errors may remain in the steady state, but they are small enough to be eliminated by subsequent channel tracking. The performance for tracking CFO and STO will deteriorate when the SNR value becomes lower. The tracking curves at a very low SNR level of 6 dB are also given for reference. The performance for CFO tracking is not poor, whereas the STO tracking curve slowly fluctuates in a wide range.

The performance of the RLS-based joint offsets estimation algorithm is evaluated in comparison with the joint weighted

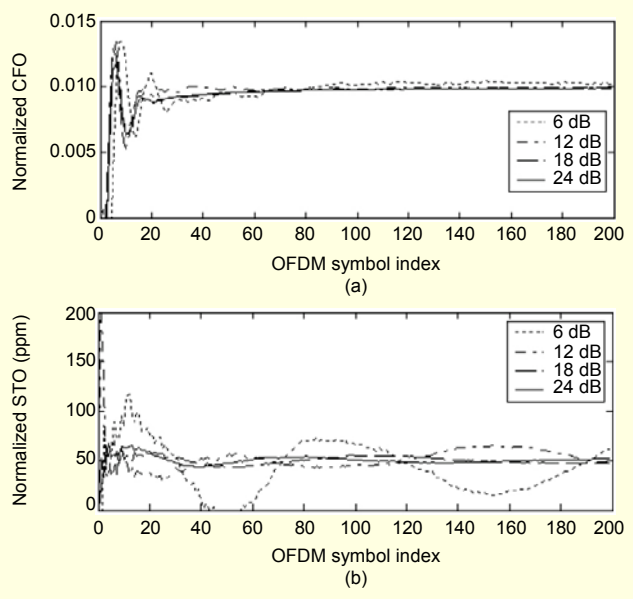

Fig. 5. Snapshot of the proposed residual synchronization error tracking performance in multipath fading channel at different SNR levels: (a) carrier frequency offset tracking curve and (b) sampling time offset tracking curve.

least-squares (WLS) line-fitting algorithm proposed in [6] and the linear least-squares (LLS) line-fitting algorithm proposed in [5]. We assume the number of OFDM symbols used for averaging N_{av} in each of the LLS and WLS algorithms is 12. The simulated estimation RMS errors by three joint estimation algorithms are shown in Fig. 6. In our simulations, the normalized residual CFO – ε is fixed at 5×10^{-3}, the normalized STO – δ is fixed at -50 ppm, and the SNR value changes from 9 dB to 33 dB. As can be seen in Fig. 6, the LLS algorithm is much poorer at estimating both offsets than the other two algorithms, and the proposed RLS estimation outperforms the WLS algorithm by achieving an RMS error reduction of 2 to 3 dB.

Finally, we investigate the overall BER performance of the proposed error elimination scheme in the multipath Rayleigh fading channel corrupted by AWGN. An SUI-4 model with no Doppler effect or a Doppler frequency of 20 Hz is used in these simulations. The whole architecture is included in a simulated 802.16d baseband transceiver system for performance evaluation. Only 16-QAM modulation is used and no coding is employed. A normalized residual CFO and a normalized STO are assumed as 0.5% and 40 ppm, respectively.

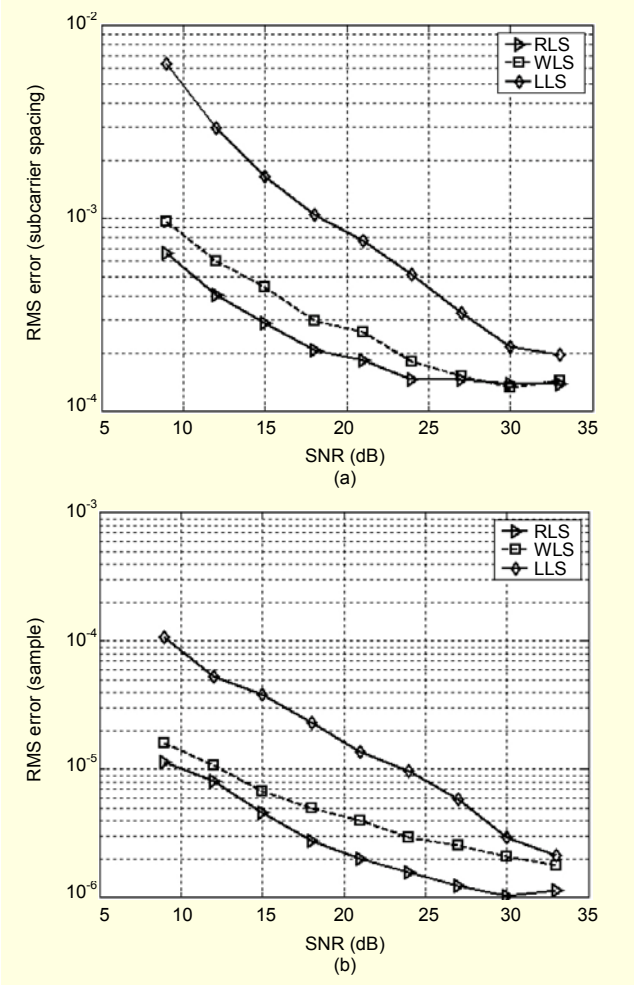

Fig. 6. Estimation RMS errors versus SNR by different algorithms in multipath channels: (a) carrier frequency offset and (b) sampling time offset.

To demonstrate the benefits of the proposed scheme, we consider three cases: full tracking (pilot-aided tracking plus effective channel gain update), partial tracking (only pilot-aided tracking), and no tracking. Especially for the full tracking case, performance comparisons are made between different OFDM receivers employing LLS, WLS, and RLS algorithms to verify the BER improvement of the proposed recursive estimation algorithms. The BER performance of an offset-free OFDM system with perfect channel knowledge is also simulated for intuitive comparison with that of systems employing full, partial, or no error tracking scheme.

Note that before the decision-directed channel tracking scheme is performed, channel coefficients are initially estimated in the following manner. First, the LS estimates of channel frequency response values are computed at even subcarriers by means of dividing the received pilot symbols by the local known pilots. Then, linear interpolation is performed between two adjacent even subcarriers to get estimates of channel coefficients at odd subcarriers. Finally, this data is sent into a finite impulse response (FIR) filter with exponential-decay power to produce smoothed estimates of channel gains at each data subcarriers.

Figure 7 shows the uncoded BER performance curves for various simulation cases mentioned above in the same multipath fading channel where there is no Doppler effect. Similarly, raw BER performances corresponding to a slow-fading channel with a 20 Hz Doppler frequency are shown in Fig. 8. As Figs. 7 and 8 demonstrate, BER performance

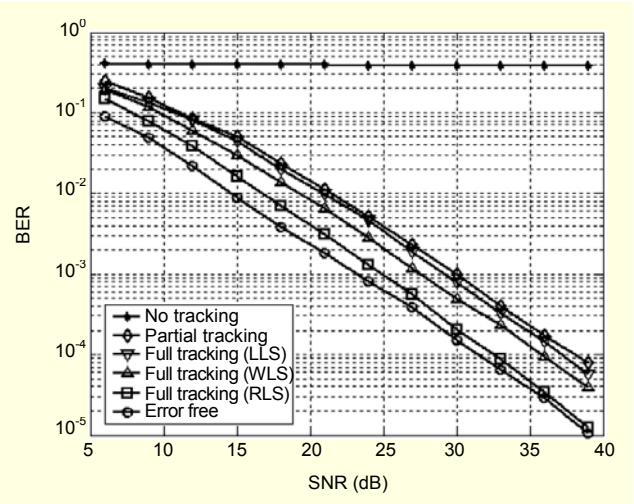

Fig. 7. Raw BER performance versus SNR of OFDM systems with and without error tracking compared with that of an offset-free system with perfect channel knowledge when the Doppler frequency is 0 Hz.

improvement on conventional schemes by adopting LLS or WLS line-fitting estimation algorithms is achieved when the proposed RLS algorithm is employed. The receiver also performs much better in the full tracking mode than in the partial tracking mode. From Fig. 7, as the Doppler frequency is set to zero, we conclude that decision-directed channel tracking can work to further improve the BER performance by effectively eliminating the tiny CFO and STO remaining after the pilot-aided tracking. As the SNR gets higher, the improvement become more obvious, and it can reach 7 to 8 dB in BER reduction at most. As shown in Figs. 7 and 8, the overall BER performance of the proposed error tracking scheme is closest to that of an OFDM system with perfect synchronization parameters, especially at high SNR levels. Finally, if there is not any tracking scheme, the performance will become terribly poor. Therefore the effectiveness of the proposed synchronization error elimination scheme has been well justified.

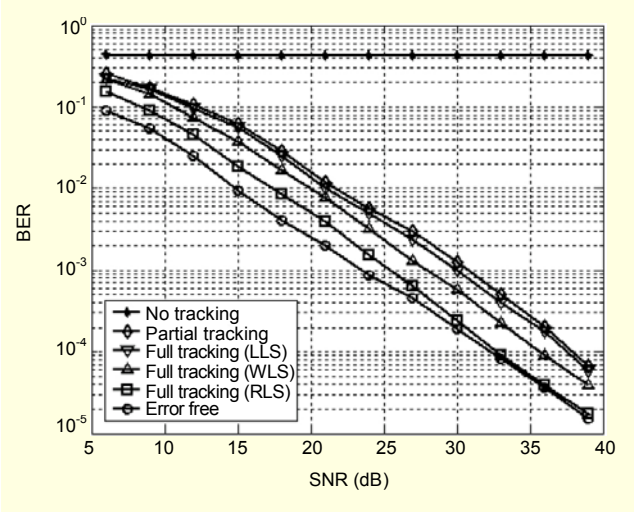

Fig. 8. Raw BER performance versus SNR of OFDM systems with and without error tracking compared with that of an offset-free system with perfect channel knowledge when the Doppler frequency is 20 Hz.

VI. Conclusion

In this paper, we proposed an efficient synchronization error elimination scheme to trace and remove the residual carrier frequency and sampling time offsets in the digital OFDM baseband receiver. Three new algorithms or techniques are devised for this scheme to achieve improvement on existing systems. A pilot-aided recursive algorithm is used for joint estimation of CFO and STO. It can achieve hardware efficiency by greatly reducing data storage and also improve estimation performance compared with conventional LS algorithms. The delay-based timing error correction directly updates the control parameters by iterative computations. It can effectively obviate the possible large sampling disturbance which could crash the signal detection. The channel tracking loop employs a new decision-directed channel gain update algorithm based on the RLS criterion, which can achieve faster convergence and smaller error than the conventional LMS algorithms. Simulation results demonstrate that the new channel updating technique can improve BER performance by eliminating tiny synchronization errors remaining even after the fine offset tracking. The effectiveness of the whole scheme has been justified by various numerical simulations and the overall BER simulation has shown that the performance of the proposed error elimination scheme is close to that of a system with perfect synchronization parameters.

Appendix. Mathematical Derivation of the Proposed Recursive Algorithm

As seen in (8), when both the carrier frequency and sampling clock offsets are present, $S_{i,k}/H_{i,k}$ will be shifted in phase as given in [6] by

$$\pi(\varepsilon+\delta k+\delta\varepsilon)[2(iN+iN_g+N_g)/N+1-1/N]. \quad \text{(A1)}$$

Since $\delta\cdot\varepsilon$ has a much smaller order of magnitude than ε or δ, this term will be ignored in the following derivation.

Assume that J pilots are inserted into N subcarriers, and these pilot subcarrier indexes are denoted by $p_j, j = 0, 1, \cdots, J\text{-}1$. Pilot data is differentially encoded with a PN-sequence which is known at the receiver, so we can have

$$X_{i,p_j} = C_{i,p_j} X_{i-1,p_j}, C_{i,p_j} \in \{+1,-1\}. \quad \text{(A2)}$$

For any $i \geq 1$ and $j \in \{0,1,\cdots,J\text{-}1\}$, compute the phase difference of the received pilot data between two consecutive OFDM symbols as given in [6] as

$$\begin{aligned}\varphi_{i,j} &= \arg(C_{i,p_j} Y_{i,p_j} Y^*_{i-1,p_j}) \\ &= \arg(C_{i,p_j} S_{i,p_j} S^*_{i-1,p_j}) + e_{i,j} \\ &= 2\pi\frac{N+N_g}{N}[p_j \quad 1]\cdot[\delta \quad \varepsilon]^T + e_{i,j},\end{aligned} \quad \text{(A3)}$$

where arg(·) is the phase of its argument, and $e_{i,j}$ is the phase rotation due to ICI and additive noise.

Prior to further derivation, we weight (A3) with a coefficient $\omega_{i,j}$:

$$\begin{aligned}\psi_{i,j} &= \omega_{i,j}\varphi_{i,j} \\ &= 2\pi\frac{N+N_g}{N}[\omega_{i,j}p_j \quad \omega_{i,j}][\delta \quad \varepsilon]^T + \omega_{i,j}e_{i,j}.\end{aligned} \quad \text{(A4)}$$

Considering that the phases of the subcarriers with little fading are more reliable than those of the deeply faded subcarriers in transmission, the coefficient ω_{ij} can be set to the LS estimate of

the channel gain of the relevant pilot subcarrier:

$$\omega_{i,j} = \left| \frac{Y_{i,p_j}}{X_{i,p_j}} \right|. \quad \text{(A5)}$$

By stacking (A4) for $j = 0, 1, \cdots, J\text{-}1$ and expressing them in vector form, we have

$$\boldsymbol{\psi}_i = \mathbf{Q}_i \mathbf{b} + \mathbf{e}_i, \quad \text{(A6)}$$

where

$$\boldsymbol{\psi}_i = [\psi_{i,0} \quad \psi_{i,1} \quad \cdots \quad \psi_{i,J-1}]^T,$$

$$\mathbf{Q}_i = \begin{bmatrix} \omega_{i,0} p_0 & \omega_{i,1} p_1 & \cdots & \omega_{i,J-1} p_{J-1} \\ \omega_{i,0} & \omega_{i,1} & \cdots & \omega_{i,J-1} \end{bmatrix}^T,$$

$$\mathbf{b} = 2\pi \frac{N + N_g}{N} [\delta \quad \varepsilon]^T,$$

$$\boldsymbol{e}_i = [\omega_{i,0} e_0 \quad \omega_{i,1} e_1 \quad \cdots \quad \omega_{i,J-1} e_{J-1}]^T.$$

The previous vector equation is based on the pilot data of the (i-1)th and i-th OFDM symbols. Thus, all of the pilots in the OFDM symbols prior to the (i+1)th symbol can be utilized to form a larger vector equation

$$\boldsymbol{\Psi}_i = \mathbf{R}_i \mathbf{b} + \mathbf{E}_i, \quad \text{(A7)}$$

where

$$\boldsymbol{\Psi}_i = [\boldsymbol{\psi}_1 \quad \cdots \quad \boldsymbol{\psi}_{i-1} \quad \boldsymbol{\psi}_i]^T,$$

$$\mathbf{R}_i = [\mathbf{Q}_1 \quad \cdots \quad \mathbf{Q}_{i-1} \quad \mathbf{Q}_i]^T,$$

$$\mathbf{E}_i = [\mathbf{e}_1 \quad \cdots \quad \mathbf{e}_{i-1} \quad \mathbf{e}_i]^T.$$

Thus, according to (A7), the LS estimate of $\mathbf{b}$ is given by

$$\hat{\mathbf{b}}_i = (\mathbf{R}_i^T \mathbf{R}_i)^{-1} \mathbf{R}_i^T \boldsymbol{\Psi}_i. \quad \text{(A8)}$$

On receiving the (i+1)th OFDM symbol, we get a new vector equation

$$\boldsymbol{\psi}_{i+1} = \mathbf{Q}_{i+1} \mathbf{b} + \mathbf{e}_{i+1}, \quad \text{(A9)}$$

or

$$\psi_{i+1,j} = \mathbf{q}_{i+1,j}^T \mathbf{b} + e'_{i+1,j} \quad (j = 0, 1, \cdots, J-1), \quad \text{(A10)}$$

where

$$\psi_{i+1,j} = \omega_{i+1,j} \varphi_{i+1,j},$$

$$\mathbf{q}_{i+1,j}^T = [\omega_{i+1,j} p_j \quad \omega_{i+1,j}],$$

$$e'_{i+1,j} = \omega_{i+1,j} e_{i+1,j}.$$

Define $\boldsymbol{\Psi}_{i+1,-1} = \boldsymbol{\Psi}_i$, $\mathbf{R}_{i+1,-1} = \mathbf{R}_i$, $\mathbf{E}_{i+1,-1} = \mathbf{E}_i$, and

$$\boldsymbol{\Psi}_{i+1,j} = [\boldsymbol{\Psi}_{i+1,-1} \quad \cdots \quad \psi_{i+1,j}]^T,$$

$$\mathbf{R}_{i+1,j} = [\mathbf{R}_{i+1,-1} \quad \cdots \quad \mathbf{q}_{i+1,j}^T]^T,$$

$$\mathbf{E}_{i+1,j} = [\mathbf{E}_{i+1,-1} \quad \cdots \quad e_{i+1,j}]^T.$$

Evaluate (A10) for $j = 0, 1, \cdots, J\text{-}1$, respectively, and add them into (A7) in turn to form new vector equations. For any $j \in \{0, 1, \cdots, J-1\}$, we have

$$\boldsymbol{\Psi}_{i+1,j} = \mathbf{R}_{i+1,j} \mathbf{b} + \mathbf{E}_{i+1,j}. \quad \text{(A11)}$$

Expand the above equation to yield

$$\begin{bmatrix} \boldsymbol{\Psi}_{i+1,j} \\ \psi_{i+1,j+1} \end{bmatrix} = \begin{bmatrix} \mathbf{R}_{i+1,j} \\ \mathbf{q}_{i+1,j+1}^T \end{bmatrix} \mathbf{b} + \begin{bmatrix} \mathbf{E}_{i+1,j} \\ e_{i+1,j+1} \end{bmatrix}, \quad \text{(A12)}$$

which can also be denoted as

$$\boldsymbol{\Psi}_{i+1,j+1} = \mathbf{R}_{i+1,j+1} \mathbf{b} + \mathbf{E}_{i+1,j+1}. \quad \text{(A13)}$$

According to the RLS algorithm, for a forgetting factor w ($0 < w < 1$), the recursive formulas for estimating $\mathbf{b}$ are given by

$$\hat{\boldsymbol{b}}_{i+1,j+1} = \hat{\boldsymbol{b}}_{i+1,j} + \boldsymbol{K}_{i+1,j+1} (\psi_{i+1,j+1} - \boldsymbol{q}_{i+1,j+1}^T \hat{\boldsymbol{b}}_{i+1,j}) \quad \text{(A14)}$$

and

$$\mathbf{V}_{i+1,j+1} = 1/w \cdot (\mathbf{V}_{i+1,j} - \mathbf{K}_{i+1,j+1} \mathbf{q}_{i+1,j+1}^T \mathbf{V}_{i+1,j}), \quad \text{(A15)}$$

where

$$\boldsymbol{K}_{i+1,j+1} = (w + \boldsymbol{q}_{i+1,j+1}^T \boldsymbol{V}_{i+1,j} \boldsymbol{q}_{i+1,j+1})^{-1} \boldsymbol{V}_{i+1,j} \boldsymbol{q}_{i+1,j+1}. \quad \text{(A16)}$$

References

[1] M. Speth, S. Fechtel, G. Fock, and H. Meyr, "Optimum Receiver Design for OFDM-Based Broadband Transmission – Part II," *IEEE Trans. Commun.*, vol. 49, no. 4, Apr. 2001, pp. 571-578.

[2] S.P. Jimenez, M.J. Garcia, F.J. Serrano, and A.G. Armada, "Design and Implementation of Synchronization and AGC for OFDM-Based WLAN Receivers," *IEEE Trans. Consum. Electron.*, vol. 50, no. 4, Nov. 2004, pp. 1016-1025.

[3] S.J. Yang, Y.C. Lei, and T.D. Chiueh, "Design and Simulation of a Baseband Transceiver for IEEE 802.16a OFDM-Mode Subscriber Stations," *Proc. 2004 IEEE Asia-Pacific Conf. on Circ. and Syst.*, vol. 2, Dec. 2004, pp. 697-700.

[4] J. Liu and J. Li, "Parameter Estimation and Error Reduction for OFDM-Based WLANs," *IEEE Trans. Mobile Computing*, vol. 3, no. 2, Apr.-June 2004, pp. 152-163.

[5] I.H. Hwang, H.S. Lee, and K.W. Kang, "Frequency and Timing Period Offset Estimation Technique for OFDM Systems," *Electron. Lett.*, vol. 34, no. 6, Mar. 1998, pp. 520-521.

[6] P.Y. Tsai, H.Y. Kang, and T.D. Chiueh, "Joint Weighted Least-Squares Estimation of Carrier-Frequency Offset and Timing Offset for OFDM Systems over Multipath Fading Channels," *IEEE Trans. Vehicular Technol.,* vol. 54, no. 1, Jan. 2005, pp. 211-223.

[7] L. Kuang, Z. Ni, J. Lu, and J. Zheng, "A Time-Frequency Decision-Feedback Loop for Carrier Frequency Offset Tracking in OFDM Systems," *IEEE Trans. Commun.,* vol. 4, no. 2, Mar. 2005, pp. 367-373.

[8] F.M. Gardner, "Interpolation in Digital Modems – Part I: Fundamentals," *IEEE Trans. Commun.,* vol. 41, no. 3, Mar. 1993, pp. 501-507.

[9] M. Speth, S.A. Fechtel, G. Fock, and H. Meyr, "Optimum Receiver Design for Wireless Broadband Systems Using OFDM – Part I," *IEEE Trans. Commun.,* vol. 47, no. 11, Nov. 1999, pp. 1668-1677.

[10] X. Wang, T.T. Tjhung, Y. Wu, and B. Caron, "SER Performance Evaluation and Optimization of OFDM System with Residual Frequency and Timing Offsets from Imperfect Synchronization," *IEEE Trans. Broadcast,* vol. 49, no. 2, June 2003, pp. 170-177.

[11] T. Pollet and M. Peeters, "Synchronization with DMT Modulation," *IEEE Comm. Mag*, vol. 37, no. 4, Apr. 1999, pp. 80-86.

[12] L. Erup, F.M. Gardner and R.A. Harris, "Interpolation in Digital Modem – Part II: Implementation and Performance," *IEEE Trans. Commun.,* vol. 41, no. 6, June 1993, pp. 998-1008.

[13] IEEE 802.16a-03/01, *IEEE Standard for Local and Metropolitan Area Networks, Part 16: Air Interface for Fixed Broadband Wireless Access Systems*, June. 2004.

[14] IEEE Std. 802.16-2004, *Channel Models for Fixed Wireless Applications*, IEEE 802.16 Broadband Wireless Access Working Group Technical Reports, 2003.

Xingbo Hu received the BS degree in electrical engineering from Wuhan University, Hubei, China, in 1998, and the MS degree in electrical engineering from Tsinghua University, Beijing, China, in 2001. He is currently working towards a PhD degree in microelectronics at Fudan University, Shanghai, China. His research interests include design and VLSI implementation for digital wireless transceivers, signal processing algorithms involved in wireless communications, and RF-baseband co-design.

Yumei Huang received the BS and MS degrees from Huazhong University of Science and Technology, Hubei, China, in 1993 and 1996, respectively, and the PhD degree from Fudan University, Shanghai, China, in 2004. She is currently an assistant professor at the Department of Microelectronics, Fudan University. Since 2002, she has participated in the development of CMOS RF transceiver and baseband circuits for Bluetooth and WLAN 802.11b/g. Her research interests include CMOS RF/analog IC and RF system design for wireless communication and high frequency noise optimization.

Zhiliang Hong received the BS degree in physics from the Chinese University of Science and Technology, Beijing, China, in 1970, and the PhD degree from ETH, Zurich, Switzerland, in 1985. Since 1996, he has been with the Department of Electronic Engineering, Fudan University, Shanghai, China, where he is currently a professor and vice director of the State Key Laboratory of ASIC and Systems. From 1992 to 1994, as a visiting scholar, he visited the Department of Information Processing of Hannover University, Germany. His research interests include high-performance analog and mixed integrated circuits design and RF system design for digital wireless communication.